

## Second-Harmonic Generation from the Surface of a Simple Metal, Al

R. Murphy, M. Yeganeh, K. J. Song, and E. W. Plummer

*Physics Department, University of Pennsylvania, Philadelphia, Pennsylvania 19104*

(Received 20 April 1989)

Quantitative measurements of the second-harmonic response of Al(111), Al(100), and polycrystalline Al to 1.06- $\mu\text{m}$  radiation under ultrahigh-vacuum conditions are presented. The results verify theoretical predictions that at low frequencies the second-harmonic response is sensitive to the charge-density profile of the surface region. The effects of band structure are clearly visible in the anisotropic second-harmonic response for appreciable field components parallel to the surface. The anisotropic response can be interpreted to give information about electronic surface states.

PACS numbers: 78.20.-e, 71.25.Pi

There has been a significant theoretical effort toward understanding the mechanism and relative magnitude of second-harmonic generation from simple metal surfaces.<sup>1-7</sup> The theoretical interest in second-harmonic generation from surfaces has been driven by the anticipation that second-harmonic generation will become a useful optical probe of the physical and chemical properties of surfaces and interfaces.<sup>8</sup> Our interest centers around the use of second-harmonic generation to probe the ground-state charge distribution of the surface at low laser frequencies and the dynamic response of the electrons at higher frequencies.<sup>9</sup>

Calculations of the second-order nonlinear response range in sophistication from classical hydrodynamic approaches<sup>1</sup> to a time-dependent local-density calculation.<sup>2-4</sup> Most of these calculations model the surfaces within the jellium approximation for which there is translational invariance parallel to the surface and a uniform bulk electronic density.

For these model surfaces the expression for the amplitude of the  $p$ -polarized second-harmonic field takes the approximate form,<sup>5</sup>

$$E_p^{2\omega} \sim \{a(\omega)E_z^2f + bE_zE_{\parallel}g + d\mathbf{E} \cdot \mathbf{E}h\} \quad (1)$$

where  $E$  is the macroscopic field inside the surface and  $E_z$  and  $E_{\parallel}$  are normal and parallel to the surface, respectively. The factors  $f$ ,  $g$ , and  $h$  involve Fresnel reflection coefficients. The bulk magnetic dipole source is given by the  $d\mathbf{E} \cdot \mathbf{E}$  term. The terms proportional to  $a$  and  $b$  result from surface currents driven perpendicular and parallel to the surface, respectively. The coefficient  $a(\omega)$  characterizing the response normal to the surface is proportional to the integral across the surface of the component of the second-order current normal to the surface. The coefficient  $b$  is similarly defined for the currents induced parallel to the surface. The bulk and parallel second-harmonic source currents are largely determined by the bulk dielectric properties. On the other hand, the second-order currents normal to the surface are very sensitive to the dynamic screening properties of the surface region.

There are significant discrepancies among the various calculations regarding the magnitude of  $a(\omega)$  for bulk electronic densities corresponding to Al. A hydrodynamic response calculation using a rigid step-function profile for the surface charge-density profile and a static input field obtained  $a(0) = -\frac{2}{9}$ .<sup>1</sup> Another hydrodynamic calculation using a smoother Lang-Kohn surface charge-density profile obtained  $a(0) = -35$ .<sup>7</sup> The most comprehensive time-dependent local-density calculation<sup>4</sup> gave  $a(0) = -30$  and  $a(\omega = 1.17 \text{ eV}) = -39 - 9i$ . The wide range of theoretical values for  $a(\omega)$  corresponds to measured intensity differences larger than  $2 \times 10^4$ . Experiments which analyzed the angular dependence of second-harmonic generation from Ag and Al indicated that  $a$  is of order  $+1.5$ .<sup>10</sup> These calculations illustrate that the second-order response normal to the surface is very sensitive to the ground-state charge-density profile in the static field limit. Understanding the magnitude and origin of the surface  $a(\omega)$  term is critical if second-harmonic generation is to become a quantitative probe of the surface.

In this paper we present the first quantitative measurements of the second-harmonic response of Al(111), Al(100), and polycrystalline Al under ultrahigh-vacuum conditions for a fundamental wavelength of 1.06  $\mu\text{m}$ . *The results show that the magnitude of the second-harmonic response in the direction normal to these Al surfaces is close to that predicted by quantum-mechanical calculations which involve a realistic description of the surface charge-density profile.*<sup>3-5</sup> *These results verify the theoretical prediction that a realistic description of the ground-state charge-density profile is necessary to obtain the response normal to the surface in the low-frequency limit.* For a smooth surface we now quantitatively understand the second-order response. We also present polarization studies at near normal incidence where the incident field is largely parallel to the surface which indicate substantial anisotropy in the second-harmonic response as a function of the input polarization angle relative to the crystal axis. This anisotropy is an indication of significant bulk

and/or surface band-structure effects not treated by the jellium calculations.<sup>8</sup> We suggest that the anisotropy observed from Al(111) may result from electric dipole coupling to a surface state.

The measurements were performed using a fundamental input beam wavelength of  $1.06 \mu\text{m}$  from a Nd-doped yttrium-aluminum-garnet laser producing 10-ns pulses at a rate of 20 Hz. The pulse energy was  $\approx 7.0 \text{ mJ}$  in a 5-mm-diam spot. The Al crystals were kept at a base pressure of  $1 \times 10^{-10}$  Torr during the measurements at room temperature. The surfaces were cleaned by  $\text{Ar}^+$  ion sputtering. The polycrystalline Al surface was prepared by evaporation of a macroscopic film of Al onto a sapphire substrate within the high-vacuum chamber. The second-harmonic intensity was calibrated against the fundamental intensity by passing a known amount of the input beam through a quartz crystal excited at a Maker fringe.<sup>11</sup> This reference provides quantitative values of the efficiency of second-harmonic generation to within approximately  $\pm 20\%$ . The error on the relative intensities between different spectra is less than 5%.

We will first discuss a determination of the  $a(\omega)$  parameter characterizing the magnitude of the second-harmonic response normal to the surface. Figure 1 shows the second-harmonic conversion efficiency for  $p$ -polarized fundamental input radiation generating  $p$ -polarized second-harmonic radiation as a function of the angle of incidence of the input beam with respect to the normal of the Al(111) crystal. The data points are shown for angles of incidence equal to  $15^\circ$ ,  $45^\circ$ ,  $60^\circ$ , and  $75^\circ$ . The solid line is the calculated conversion efficiency using the  $a(\omega = 1.17 \text{ eV})$  value  $-36 - 9i$  ( $b = -1, d = 1$ ) of the time-dependent local-density-functional calcula-

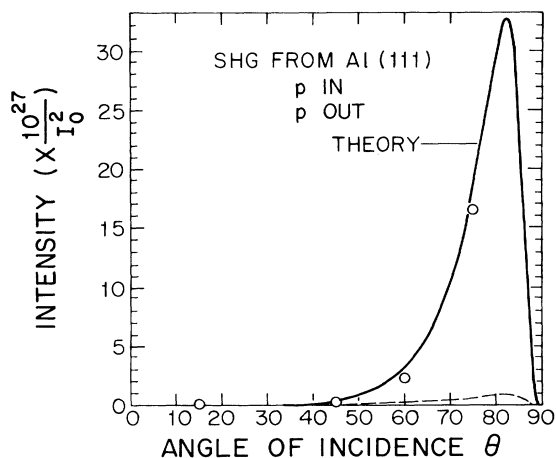


FIG. 1. Al(111) second-harmonic conversion efficiency ( $\text{cm}^2\text{sec/erg}$ ) for  $p$ -polarized fundamental and  $p$ -polarized second harmonic vs the angle of incidence with respect to the crystal normal. The experimental intensity scale has an associated  $\pm 20\%$  error not displayed. The solid line is the  $a = -36 - 9i$  time-dependent local-density result (Ref. 4).

tions.<sup>4</sup> The dashed line is the conversion efficiency for  $a = -1$  characteristic of a less-polarizable surface electronic density. In Fig. 2 we show the  $p$ -polarized second-harmonic conversion efficiency for Al(111) versus the input polarization angle for a  $75^\circ$  angle of incidence. The peak intensity occurring at  $p$  input polarization in Fig. 2 corresponds to the most intense experimental point in Fig. 1. The upper solid line is the  $a = -36 - 9i$  local-density result<sup>4</sup> while the lower line is the  $a = -1$  result. For these two experiments there is reasonable agreement between the second-harmonic intensity and the time-dependent local-density results. We note that this experiment does not give a definitive assignment of the phase of  $a(\omega)$  since the data can also be fitted well with  $a = -37$ . The  $a = -1$  result is clearly an underestimate of the response. These results clearly indicate that *the second-harmonic response normal to the surface is quite sensitive to the surface charge-density profile at low frequencies. The surface currents normal to the surface dominate the second-harmonic response for appreciable components of the field normal to the surface.* We note that the value of  $a \approx +1.5$  obtained experimentally by Quail and Simon<sup>10</sup> is not comparable to our data since their data were not taken under high-vacuum conditions and with a less direct optical arrangement.

Figure 3 shows the conversion efficiency versus angle of incidence for all of the Al surfaces studied as in Fig. 1. There is approximately a factor of 3 decrease in the second-harmonic intensity obtained from Al(100) and polycrystalline Al relative to Al(111). The Al(100) and polycrystalline Al intensities correspond to  $a \approx -22$ . The relative decrease in the intensities between Al(111) and Al(100) implies that the response of the surface re-

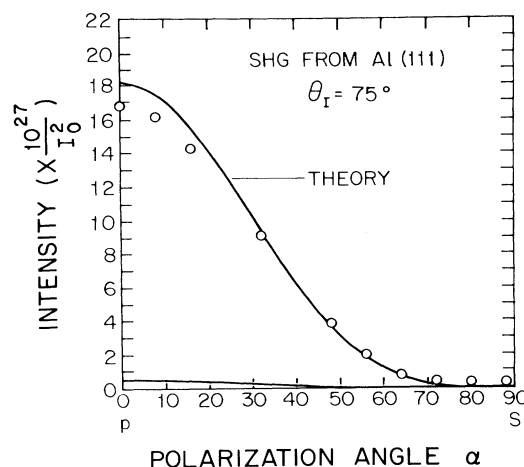


FIG. 2. Al(111) second-harmonic conversion efficiency ( $\text{cm}^2\text{sec/erg}$ ) for  $p$ -polarized second harmonic vs the polarization of the fundamental beam. The angle of incidence is  $75^\circ$ . The solid line is the  $a = -36 - 9i$  time-dependent local-density result (Ref. 4).

gion depends upon the total nuclear potential felt by the surface electronic density which is certainly different between the (111) and (100) surfaces. The lower response for the (100) surface could simply mean that the nuclear potential of the (100) surface is on average stronger than the potential of the (111) surface thus decreasing the response. The stronger nuclear potential of the (100) surface could be a result of the larger corrugation of a more open surface. Some theoretical support for the argument that the nuclear potentials can decrease the response comes from a calculation by Aers and Inglesfield of the second-order response of Ag(100) to a static field.<sup>12</sup> Using an embedded-atom band structure for Ag(100) it was found that  $a(0)$  is a factor of 3 smaller than the corresponding local-density-functional result<sup>2</sup> for an equivalent electron density.

Although the second-harmonic response normal to the Al surfaces seems to be modeled fairly well by jellium local-density-functional approaches, we have found significant effects of band structure in the second-harmonic response for a 15° angle of incidence. In Fig. 4 we plot the  $p$ -polarized second-harmonic yields from Al(111) at an angle of incidence of 15° versus the polarization of the fundamental beam. The crystal is oriented such that the electric field vector for  $s$  input polarization is along the  $[11\bar{2}]$  direction which bisects a set of (111) surface triangles. The larger peaks in the spectrum result from  $p$  input polarization and the less intense central peak occurs at  $s$  input polarization where the incident

field has the largest component parallel to the surface. The square of the incident field component normal to the surface is a factor of 14 smaller than that corresponding to the equivalent 75° angle-of-incidence spectrum of Fig. 2. The peak at  $s$  polarization decreases in intensity as the angle of incidence is increased to the point that at an angle of incidence of 60° the peak is just visible. At a 75° angle of incidence the peak at  $s$  polarization is not visible relative to the scale of the peaks at  $p$  input resulting from the normal response as shown in Fig. 2. When the crystal was rotated about the axis normal to the crystal by 10° and 20°, at the 15° angle-of-incidence geometry, the peak positions defined by the input polarization angles shifted nearly linearly with the crystal rotation.

These results indicate that most of the response at this low angle of incidence is from anisotropic source terms where the anisotropic terms depend upon the relative orientation of the crystal axis to the input polarization direction. These anisotropic terms are clearly neglected in the jellium approximations which explains why the theoretical intensity for  $a = -36 - 9i$  shown in Fig. 4 is too low at this small angle of incidence.

Sipe, Moss, and van Driel<sup>13</sup> have developed a phenomenological theory which accounts for anisotropic response from the anisotropic bulk electric quadrupole term and surface electric dipole terms which result whenever inversion symmetry is broken at the surface. For excitation by  $s$ -polarized fundamental and selecting  $p$ -polarized second-harmonic radiation as at the central peak position in Fig. 4, the expression for the second-

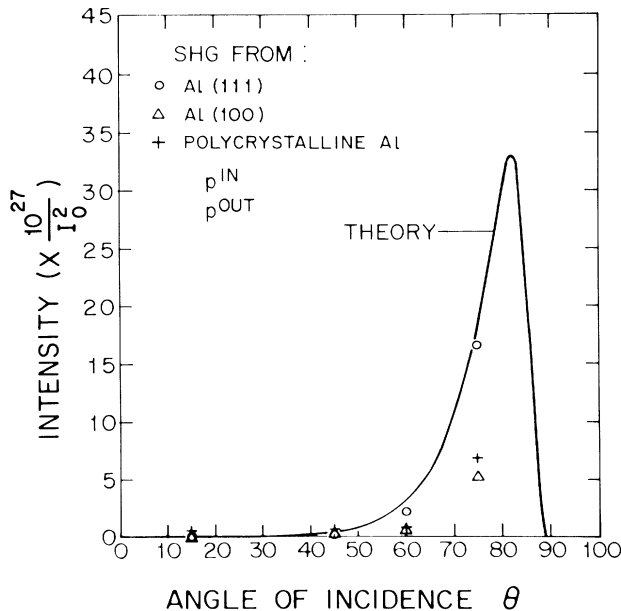


FIG. 3. Al(111), Al(100), and polycrystalline Al second-harmonic conversion efficiency ( $\text{cm}^2\text{sec/erg}$ ) for  $p$ -polarized fundamental and  $p$ -polarized second harmonic vs the angle of incidence with respect to the crystal normal.

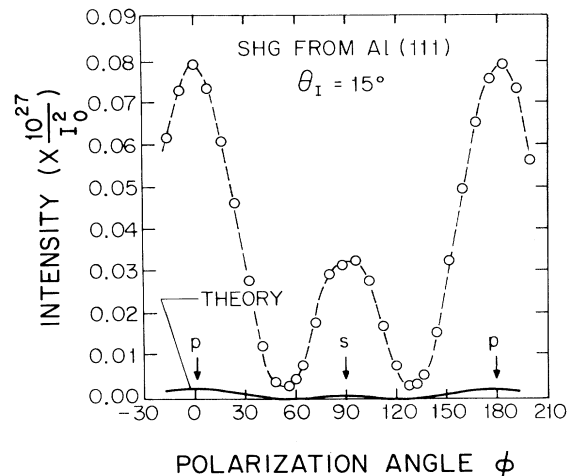


FIG. 4. Al(111) second-harmonic conversion efficiency ( $\text{cm}^2\text{sec/erg}$ ) for  $p$ -polarized second harmonic vs the polarization of the fundamental beam. The angle of incidence is 15°. The peak at  $s$  input is indicative of anisotropic response. The solid line is the  $a = -36 - 9i$  time-dependent local-density result (Ref. 4).

harmonic field from a (111) surface is<sup>13</sup>

$$E_p^{2\omega} \sim \{f\xi + [g\xi + h\chi_{\eta\eta\eta}]\cos(3\phi)\}E_s^2. \quad (2)$$

The factors  $f, g, h$  involve Fresnel reflection coefficients as functions of the bulk dielectric function.  $E_s$  is the fundamental  $s$ -polarized field.  $\phi$  is the angle that the input polarization makes with respect to the  $[11\bar{2}]$  axis denoted by  $\eta$  which bisects the triangles formed by the first layer of (111) atoms. Inversion symmetry is broken along the  $\eta$  axis when second-layer atoms are considered, thus generating via electric dipole coupling the  $\chi_{\eta\eta\eta}\cos(3\phi)$  term in  $E^{2\omega}$ . The terms proportional to  $\xi$  result from the bulk anisotropic electric quadrupole response.

Thus the intensity seen at low angles of incidence is largely from the surface dipole and/or bulk anisotropic electric quadrupole terms. The relative contribution of the anisotropic electric quadrupole term can be determined by looking at the  $s$ -polarized second-harmonic output from a (100) surface for  $p$ -polarized input as a function of the input polarization at normal incidence.<sup>8,13</sup> Lacking a full crystal rotation ability we could not obtain  $\xi$  in this manner.

We will now consider the possibility that the anisotropy results largely from the electric dipole term along the  $\eta$  direction in the (111) plane. Both band-structure calculations<sup>14</sup> and photoemission measurements<sup>15</sup> have found a surface state on Al(111) at the zone boundary  $K$  with little dispersion along the  $\Gamma$ -to- $K$  direction in the surface Brillouin zone with the surface state lying 0.58 eV below the Fermi level at  $K$ . The charge density of this surface state at  $K$  as plotted in Ref. 14 is largely within the triangular hollows of the first two (111) surface layers and shows the broken inversion symmetry characteristic of the  $\eta$  direction. It is plausible that the major contribution to the electric dipole susceptibility  $\chi_{\eta\eta\eta}$  [Eq. (2)] comes from electric dipole coupling to this occupied surface state. The character of the final and intermediate states involved in this dipole coupling are

presently unresolved; however, a frequency-dependent study of the anisotropy would help to clarify this.

This work was partially supported by NSF Grant No. DMR-8610491. The laser facility was funded by the NSF, Materials Research Laboratory program DMR-8519059. R. Murphy would like to acknowledge the support of an AT&T scholarship.

<sup>1</sup>W. L. Schaich and A. Liebsch, Phys. Rev. B **37**, 6187 (1988).

<sup>2</sup>M. G. Weber and A. Liebsch, Phys. Rev. B **35**, 7411 (1987).

<sup>3</sup>A. Liebsch, Phys. Rev. Lett. **61**, 1233 (1988).

<sup>4</sup>A. Liebsch and W. L. Schaich, Phys. Rev. B (to be published).

<sup>5</sup>J. Rudnick and E. A. Stern, Phys. Rev. B **4**, 4274 (1971).

<sup>6</sup>J. E. Sipe, Surf. Sci. **84**, 75 (1979).

<sup>7</sup>A. Chizmeshya and E. Zaremba, Phys. Rev. B **37**, 2805 (1988).

<sup>8</sup>H. W. K. Tom and G. D. Aumiller, Phys. Rev. B **33**, 8818 (1986); H. W. K. Tom, T. F. Heinz, and Y. R. Shen, Phys. Rev. Lett. **51**, 1983 (1983); H. W. K. Tom, G. D. Aumiller, and C. H. Brito-Cruz, Phys. Rev. Lett. **60**, 1438 (1988); T. F. Heinz, M. M. T. Loy, and W. A. Thompson, J. Vac. Sci. Technol. B **3**, 1467 (1985); Y. R. Shen, Nature (London) **337**, 519 (1989).

<sup>9</sup>K. J. Song, D. Heskett, H. L. Dai, A. Liebsch, and E. W. Plummer, Phys. Rev. Lett. **61**, 1380 (1988).

<sup>10</sup>J. C. Quail and H. C. Simon, Phys. Rev. B **31**, 4900 (1985).

<sup>11</sup>J. Jerphagnon and S. K. Kurtz, J. Appl. Phys. **41**, 1667 (1970).

<sup>12</sup>G. C. Aers and J. E. Inglesfield, SERC Daresbury Laboratory report, 1988 (to be published).

<sup>13</sup>J. E. Sipe, D. J. Moss, and H. M. van Driel, Phys. Rev. B **35**, 1129 (1987).

<sup>14</sup>D. Wang, A. J. Freeman, J. Krakauer, and M. Posternak, Phys. Rev. B **23**, 1685 (1981); J. R. Chelikowsky, M. Schluter, S. G. Louie, and M. L. Cohen, Solid State Commun. **17**, 1103 (1975).

<sup>15</sup>S. D. Kevan, N. G. Stoffel, and N. V. Smith, Phys. Rev. B **31**, 1788 (1985).